中国光学（中英文） Chinese Optics 核心期刊

同时测试波导传输损耗和弯曲损耗的方法

范作文 贾连希 李赵一 周敬杰 丛庆宇 曾宪峰

Method for the simultaneous measurement of waveguide propagation loss and bending loss

FAN Zuo-wen, JIA Lian-xi, LI Zhao-yi, ZHOU Jing-jie, CONG Qing-yu, ZENG Xian-feng

引用本文:
范作文, 贾连希, 李赵一, 周敬杰, 丛庆宇, 曾宪峰. 同时测试波导传输损耗和弯曲损耗的方法[J]. 中国光学, 2023, 16(5): 1177-1185. doi: 10.37188/CO.EN.2022-0027
FAN Zuo-wen, JIA Lian-xi, LI Zhao-yi, ZHOU Jing-jie, CONG Qing-yu, ZENG Xian-feng. Method for the simultaneous measurement of waveguide propagation loss and bending loss[J]. *Chinese Optics*, 2023, 16(5): 1177-1185. doi: 10.37188/CO.EN.2022-0027

在线阅读 View online: https://doi.org/10.37188/CO.EN.2022-0027

文章编号　2097-1842(2023)05-1177-09

Method for the simultaneous measurement of waveguide propagation loss and bending loss

FAN Zuo-wen[1], JIA Lian-xi[1,2,3]*, LI Zhao-yi[1], ZHOU Jing-jie[1], CONG Qing-yu[1], ZENG Xian-feng[2]
(1. *Microelectronics Institute*, *Shanghai University*, *Shanghai* 201800, *China*;
2. *Shanghai Institute of Microsystems and Information Technology*, *Chinese Academy of Sciences*, *Shanghai* 201800, *China*;
3. *Shanghai Industrial μTechnology Research Institute*, *Shanghai* 201800, *China*)
* *Corresponding author*, *E-mail*: *jialx@mail.sim.ac.cn*

Abstract: The propagation loss of a waveguide is a key indicator to evaluate the performance of an integrated optical platform. The commonly used cut-back method for measuring propagation loss requires the introduction of the spiral test structure. In order to remove bending loss, the bending radius is usually designed to be larger but this consequently has a larger footprint. In this paper, we suggested a method to simultaneously measure the propagation loss and bending loss of waveguides with a cut-back structure. According to simulations, the bending loss can be exponentially fitted with the bending radius, which can be further simplified as linear fitting between the natural logarithm of the bending loss and bending radius. A genetic algorithm was used to fit the insertion loss curve of the cut-back structure and the propagation losses and bending loss were calculated. With this method, we measured a cut-back structure of lithium niobate waveguide and got a propagation loss of 0.558 dB/cm and a bending loss of 0.698 dB/90° at a radius of 100 μm and wavelength of 1 550 nm. Using this method, we can simultaneously measure waveguide propagation loss and bending loss while mitigating the footprint.

Key words: propagation loss; bending loss; lithium niobate; genetic algorithm

同时测试波导传输损耗和弯曲损耗的方法

范作文[1], 贾连希[1,2,3]*, 李赵一[1], 周敬杰[1], 丛庆宇[1], 曾宪峰[2]
(1. 上海大学 微电子学院, 上海 201800;
2. 中国科学院 上海微系统与信息研究所, 上海 201800;
3. 上海新微技术工业研究院, 上海 201800)

摘要: 波导的传输损耗是评价集成光学平台性能的一个关键指标。常用的测量传输损耗的 cut-back 测试方法需引入弯曲波导测试结构。为了去除弯曲损耗的影响, 通常会将弯曲半径设计的足够大, 但这样会占用很多的版图面积。本文基

收稿日期: 2022-11-27; **修订日期:** 2023-01-30
基金项目: 国家重点研发计划(No. 2018YFB2200500)
Supported by the National Key Research and Development Program of China (No. 2018YFB2200500)

于铌酸锂平台提出了一种可以同时测试波导传输损耗和弯曲损耗的方法。通过仿真发现波导弯曲损耗与弯曲半径成指数关系，对弯曲损耗取对数值后，与弯曲半径成线性关系。利用遗传算法拟合 cut-back 结构的插入损耗曲线，并计算得到波导的传输损耗和弯曲损耗。用该方法测量铌酸锂波导，在 1550 nm 波长下得到 0.558 dB/cm 的传输损耗和 100 μm 弯曲半径下 0.698 dB/90°的弯曲损耗。利用这种方法可以同时测试波导的传输损耗和弯曲损耗，还可以大大节省占地面积。

关 键 词: 传输损耗；弯曲损耗；铌酸锂；遗传算法

中图分类号: TN252 **文献标志码:** A **doi:** 10.37188/CO.EN.2022-0027

1 Introduction

Recently, lithium niobate (LN) has been widely used in integrated optics and other fields due to its wide transparent window (350 nm−5 μm) and high electro-optical coefficient[1-4]. The conventional bulk LN waveguide (WG) formed by Ti diffusion has a low refractive index contrast and weak confinement to the optical field, which restricts the miniaturization of devices. The advent of LN on an insulator (LNOI) has greatly expedited the development of LN platforms[5]. LNOI retains the advantages of a bulk LN but has higher refractive index contrast, which greatly reduces the optical field and promotes the miniaturization of devices[6-7]. LNOI has been used on many integrated optical devices such as nonlinear devices, micro-ring resonators, multimode interference couplers (MMI), electro-optical modulators (EOM), optical frequency combs[8-13] etc. Cai Lutong *et al.*[14] used a proton exchange without anneal to fabricate a waveguide with a 0.16 μm exchange depth and a 2 μm width on 0.6 μm thick x-cut lithium niobate films, which had a propagation loss of 0.2 dB/cm at 1550 nm. The fabricated Y-junction based on the low-loss waveguide is shorter than the conventional Ti-diffused and proton exchanged in bulk lithium niobate, which would benefit the development of highly efficient photonic devices. Cai Lutong *et al.*[15] also used the annealed proton exchange to fabricate a waveguide with a 4 μm width on 0.56 μm thick x-cut single-crystal lithium niobate films, which had a propagation loss of 0.6 dB/cm at 1550 nm. Hu Hui *et al.*[16] etched a 2 μm wide waveguide on lithium niobate film using Ar milling and found the waveguide has a propagation loss of 6.3 dB/cm (TE mode) and 7.5 dB/cm (TM mode). Inna Krasnokutska *et al.*[17] fabricated optical waveguides using a mixture of trifluoromethane and argon gas to etch lithium niobate films with a resulting propagation loss of 0.4 dB/cm, while the slope angle of the waveguide was only 15°. In this method, the reaction between fluorine ions and lithium niobate generates a layer of lithium fluoride during the etching process[18], which makes it difficult to obtain high-quality deeply etched optical waveguides on lithium niobate films.

As a new platform of integrated optics, the propagation loss of the waveguide is the key specification to estimate its performance and the common method to measure the propagation loss is the cut-back method[19]. A cut-back structure is typically composed of several waveguides of different lengths and a spiral structure is usually used to form different lengths, which can greatly reduce the resulting footprint. Typically, the bending radius of the spiral is large enough to guarantee that the bending loss is negligible, and the insertion loss of each waveguide only includes coupling loss and propagation loss. Because the coupler of each waveguide is identical, the coupling loss is the same for each waveguide while the insertion loss of the waveguide is linear with the length of the waveguide. By fitting the insertion loss of the cut-back structure, we can get a straight line where the slope of the straight line is the propagation loss and the intercept is the coupling loss. Gutierrez A M *et al.*[20] measured waveguide propagation loss based on the analysis of the transmission spectra of asymmetric Mach-Zehnder Interferometers (MZIs). They used

this method to avoid the variation of the coupling loss of different waveguides. Sareh Taebi *et al.*[21] modified the Fabry-Perot interferometer method to measure waveguide loss. They used a superluminescent diode to excite the waveguide and fitted it with various input powers. Yiming He *et al.*[22] used the reflected spectrum of a waveguide structure to calculate waveguide loss. They analyzed the reflected interferometric pattern from the Fabry-Perot cavity to get the waveguide loss, which also avoided the coupling error. However, for waveguides with weak confinement, the radius may need to be several hundred micrometers or larger and occupy a large area even with a spiral structure, which will increase the cost of an LNOI platform remarkably due to the high price of the LNOI wafer.

Genetic algorithm (GA) is a method to search for the optimal solution by simulating the natural evolutionary process, which was first proposed by John Holland[23] in the early 1970s, and has been widely used in the field of engineering through the exploration and innovation of many scholars[24-25]. By drawing on the theory of biological evolution, GA transforms the problem to be solved into a process of biological evolution by treating the multiple solutions of the problem as a population. One solution situation after each optimization is represented as an individual in the population, and the coding of the variables to be solved as an operation on the genes in the chromosome. By changing the traits of the population (the value of the function to be solved) through the operation of selection, crossover and mutation of biological genes, the best individuals are continuously retained in the evolutionary process based on the principle of superiority and inferiority, and finally, the most suitable population is obtained by simulating the evolution of organisms in a continuously iterative way. The GA has been widely used for solving optimization problems with its superior stability and global search capability. Hence, we suggest a method based on GA to simultaneously measure the bending loss, propagation loss and coupling loss with a cut-back structure.

2 Fabrication and structure analysis

The LN waveguide is fabricated on a 6-on-8 LNOI waveguide with 0.4-μm thick top LN, 3-μm thick SiO_2 and 500-μm thick high-resistivity silicon substrate. The fabrication process is shown in Fig. 1 (color online). All fabrication processes are performed at the Shanghai Industrial μTechnology Research Institute (SITRI). The devices and components are provided by SITRI. Firstly, 0.5 μm SiO_2 was deposited by PECVD as a hard mask, then the hard mask and LN underwent lithography and etching to realize a depth of 0.1 μm. The photoresist and hard mask were removed separately. Finally, 1 μm SiO_2 was deposited as the upper cladding layer by PECVD. The scanning electron microscope (SEM) image of the LN waveguide is shown in Fig. 2 where the vertical and smooth sidewall is clearly formed.

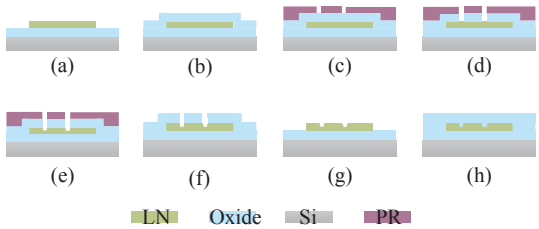

Fig. 1 Process flow of LN waveguide fabrication. (a) LNOI substrate. (b) Deposition of oxide by PECVD. (c) I-line lithography. (d) Hard mask etching. (e) LN etching. (f) Photoresist removal. (g) Hard mask removal. (h) Deposition of cladding by PECVD

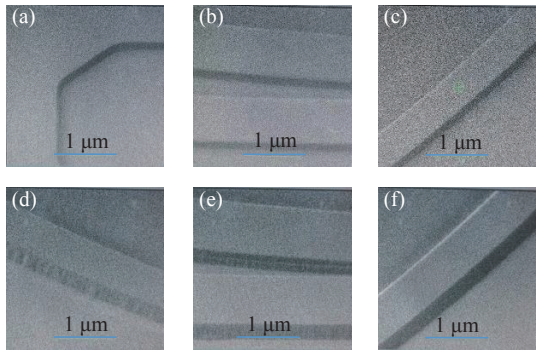

Fig. 2 The SEM image of the fabricated LN waveguide

The cut-back structure we used is comprised of five spiral waveguides with different lengths as

shown in Fig. 3. The grating coupler was used to couple with fiber and the radius and number of bends in each waveguide were different. The related information is summarized in Table 1.

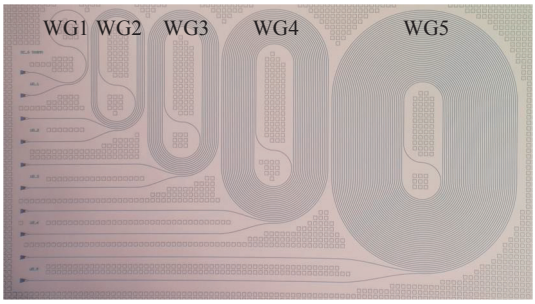

Fig. 3 The optical microscope image of the cut-back structure

Tab. 1 The basic information of the cut-back structure

	Length(cm)	The radius of bend(μm)	Number of radius
WG1	0.1582	100, 110	100×4,110×2
WG2	0.9021	100,110,120,130,140,150	(100-140)×4,150×2
WG3	2.2054	100,110,120…190,200	(100-190) ×4,200×2
WG4	5.2274	100,110,120…290,300	(100-290) ×4,300×2
WG5	11.4854	100,110,120…490,500	(100-490) ×4,500×2

Since this was the first time we fabricated an LN waveguide, to guarantee the grating coupler could work normally, we added 5 splits to the grating coupler's design (GC1-GC5) and applied them to 5 sets of cutback structures as shown in fig. 4.

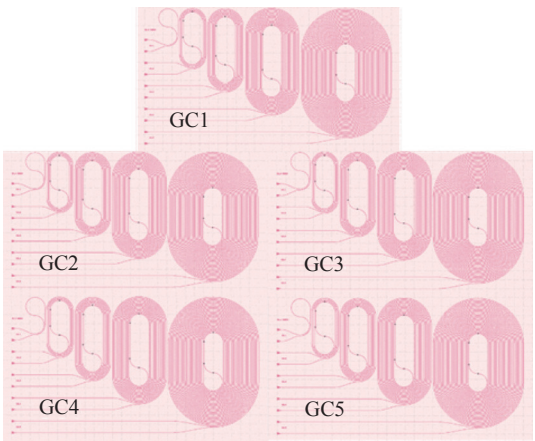

Fig. 4 Layout image of the 5 sets of cutback structures for the 5 splits of the grating coupler

3 Theory and waveguide loss analysis

The bending loss is mainly caused by the mode mismatch between a straight waveguide and a curved waveguide[26-28]. A larger radius will lead to a lower bending loss. Firstly, we simulated the bending loss of the LN waveguide with different bending radii by the Finite Difference Time Domain (FDTD) of Ansys-Lumerical. To maintain consistency with the fabricated waveguide, we chose a 90-degree LN waveguide bend with an LN thickness of 0.3 μm surrounded by 3 μm of SiO_2. The etching depth of the LN waveguide was 0.1 μm with a 72° sidewall angle, and the waveguide width was set to 1.5 μm with a simulation wavelength of 1.55 μm. The results are shown in Fig. 5(a). We found that the bending loss can be exponentially fitted with the bending radius, which can be further simplified as

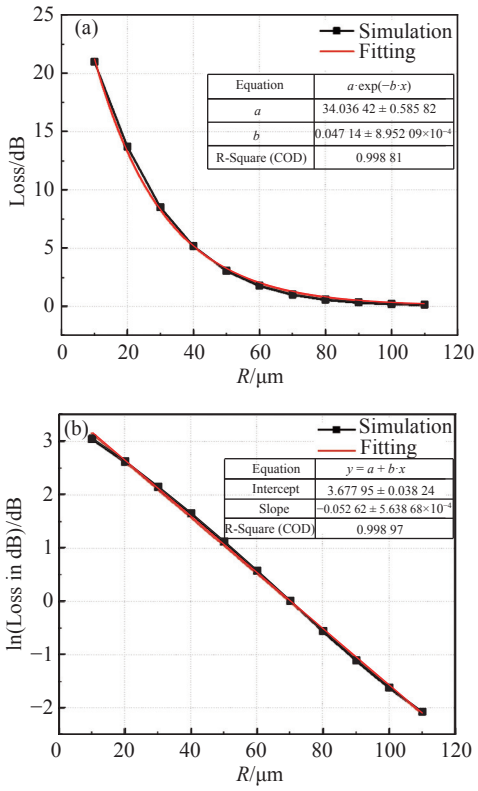

Fig. 5 (a) Simulation of the bending loss of the LN waveguide. The bending loss of the waveguide is exponentially related to the bending radius. (b) The linear fitting of the natural logarithm of the bending loss with the bending radius

linear fitting between the natural logarithm of the bending loss and the bending radius, as shown in fig. 5(b). We came to the same conclusion by simulating the LN waveguide with bends of different thicknesses, widths and sidewall angles. Therefore, the bending loss at any radius can be simply expressed assuming that the slope of the curve and the bending loss at a fixed radius are known. Then, to calculate the insertion loss of the waveguide, we only need to know four parameters: propagation loss, initial bending loss at a fixed bending radius, slope of the bending loss fitting curve and coupling loss. With the measurement results of the cut-back structure, these four parameters can be fitted iteratively. In the following sections, we will express the details of the method and successfully apply it to the characterization of the newly fabricated LNOI waveguide.

As mentioned above, the natural logarithm of the waveguide bending loss is linearly related to the bending radius, so, if we assume the bending loss at radius R_0 is α_{b0} and the slope of the linear curve is k, then the bending loss at random radius R can be expressed as:

$$\ln(\alpha_{bR}) = \ln(\alpha_{b0}) - k(R - R_0) \quad , \qquad (1)$$

Where α_{bR} is the bending loss at radius R, it can be further expressed as:

$$\alpha_{bR} = e^{\ln(\alpha_{b0}) - k(R - R_0)} \quad . \qquad (2)$$

Then, the total insertion loss α_{ti} of the waveguide can be expressed as:

$$\alpha_{ti} = \alpha_{pi} + \alpha_{bi} + \alpha_{gc} \quad , \qquad (3)$$

where α_{pi} is the propagation loss of the waveguide, α_{bi} is the bending loss, and α_{gc} is the coupling loss (i from 1 to 5, representing five waveguides, respectively). Because the grating coupler of each waveguide is identical, we can use the same coupling loss from WG1 to WG5 under the same fabrication conditions. The propagation loss is

$$\alpha_{pi} = \alpha \times L_i \quad , \qquad (4)$$

where α is the propagation loss coefficient of the waveguide (in dB/cm), and L_i is the length of the i-th waveguide (see Table 1 for specific values).

The bending loss α_{bi} is the sum of the losses of all the bends. Since our bending radii all start from 100 μm, R_0 is set to 100 μm. The bending losses of other bends can be derived from Eq (2). Thus, the total insertion loss of different waveguides can be derived:

$$\alpha_{t1} = \alpha \times L_1 + 4 \times \alpha_{b0} + 2 \times e^{\ln(\alpha_{b0}) - 10k} + \alpha_{gc} \quad , \qquad (5)$$

$$\alpha_{t2} = \alpha \times L_2 + 4 \times [\alpha_{b0} + e^{\ln(\alpha_{b0}) - 10k} + e^{\ln(\alpha_{b0}) - 20k} + e^{\ln(\alpha_{b0}) - 30k} + e^{\ln(\alpha_{b0}) - 40k}] + 2 \times e^{\ln(\alpha_{b0}) - 50k} + \alpha_{gc} \quad , \qquad (6)$$

$$\alpha_{t3} = \alpha \times L_3 + 4 \times [\alpha_{b0} + e^{\ln(\alpha_{b0}) - 10k} + e^{\ln(\alpha_{b0}) - 20k} + e^{\ln(\alpha_{b0}) - 30k} + \cdots + e^{\ln(\alpha_{b0}) - 80k} + e^{\ln(\alpha_{b0}) - 90k}] + 2 \times e^{\ln(\alpha_{b0}) - 100k} + \alpha_{gc} \quad , \qquad (7)$$

$$\alpha_{t4} = \alpha \times L_4 + 4 \times [\alpha_{b0} + e^{\ln(\alpha_{b0}) - 10k} + e^{\ln(\alpha_{b0}) - 20k} + e^{\ln(\alpha_{b0}) - 30k} + \cdots + e^{\ln(\alpha_{b0}) - 180k} + e^{\ln(\alpha_{b0}) - 190k}] + 2 \times e^{\ln(\alpha_{b0}) - 200k} + \alpha_{gc} \quad , \qquad (8)$$

$$\alpha_{t5} = \alpha \times L_5 + 4 \times [\alpha_{b0} + e^{\ln(\alpha_{b0}) - 10k} + e^{\ln(\alpha_{b0}) - 20k} + e^{\ln(\alpha_{b0}) - 30k} + \cdots + e^{\ln(\alpha_{b0}) - 380k} + e^{\ln(\alpha_{b0}) - 390k}] + 2 \times e^{\ln(\alpha_{b0}) - 400k} + \alpha_{gc} \quad . \qquad (9)$$

Since different waveguides have the same waveguide cross section and grating coupler, their propagation loss coefficient α and coupling loss α_g are the same. Therefore, there are four unknown parameters, α, α_{b0}, k and α_{gc} in the five Eqs. (5)-(9). Theoretically, we can get the solution of the four parameters if we can calculate the insertion loss of the five waveguides.

4 Fitting methods and results

To solve the four parameters, GA is used to fit the test results. The core elements of GA include parameter coding, setting of the initial population, design of the fitness function, design of the genetic operation, and setting the control parameters. The specific genetic process is shown in Fig. 6.

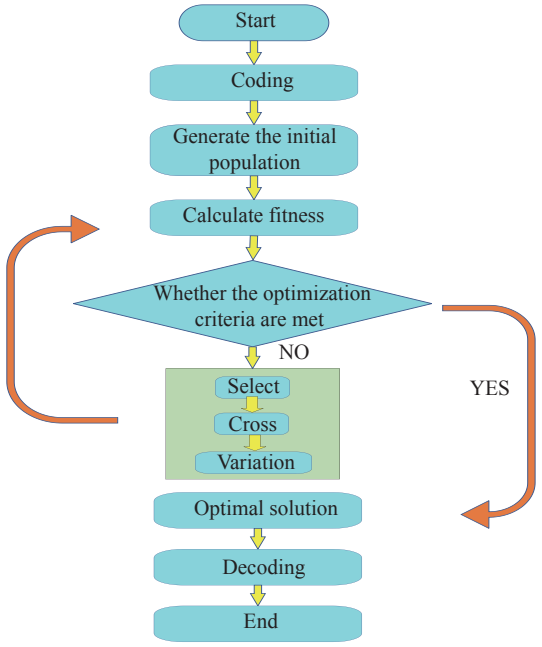

Fig. 6 The basic process of the genetic algorithm

For our situation, a set of pre-set solutions of the four unknown parameters comprised the population of the algorithm. The square root r of the calculated insertion loss α_t and the measured insertion loss α_T is

$$r = \sqrt{\begin{matrix}(\alpha_{t1}-\alpha_{T1})^2+(\alpha_{t2}-\alpha_{T2})^2+(\alpha_{t3}-\alpha_{T3})^2+\\(\alpha_{t4}-\alpha_{T4})^2+(\alpha_{t5}-\alpha_{T5})^2\end{matrix}}, \tag{10}$$

which is used as the criterion of parameter optimization. A smaller *r-value* means better matching between the fitting results and measured results so we hope to get the smallest *r-value*. In this way, we can get more accurate propagation loss and bending loss. The measured insertion loss and fitting results are compared in Fig. 7. A total of 5 sets of cut-back structures with different GCs were measured and the fifth group was tested twice due to the high loss of that GC. All the fitting results are summarized in Table 2. The fitting curves closely matched the measurement results showing that our method is effective for simultaneously measuring the propagation loss, bending loss and coupling loss. It can be seen from Table 2 that the best fitting is for the GC3 structure with an r value of 0.044, corresponding to a waveguide propagation loss of 0.558 dB/cm, bending loss of 0.698 dB/90° at a radius of 100 μm and a coupling loss of 10.74 dB. Each of these numbers is reasonable compared with results in other literatures[10, 29-32]. In this way, we simultaneously get waveguide propagation loss, bending loss, and coupling loss. The comparison of different measurement methods is shown in Table 3.

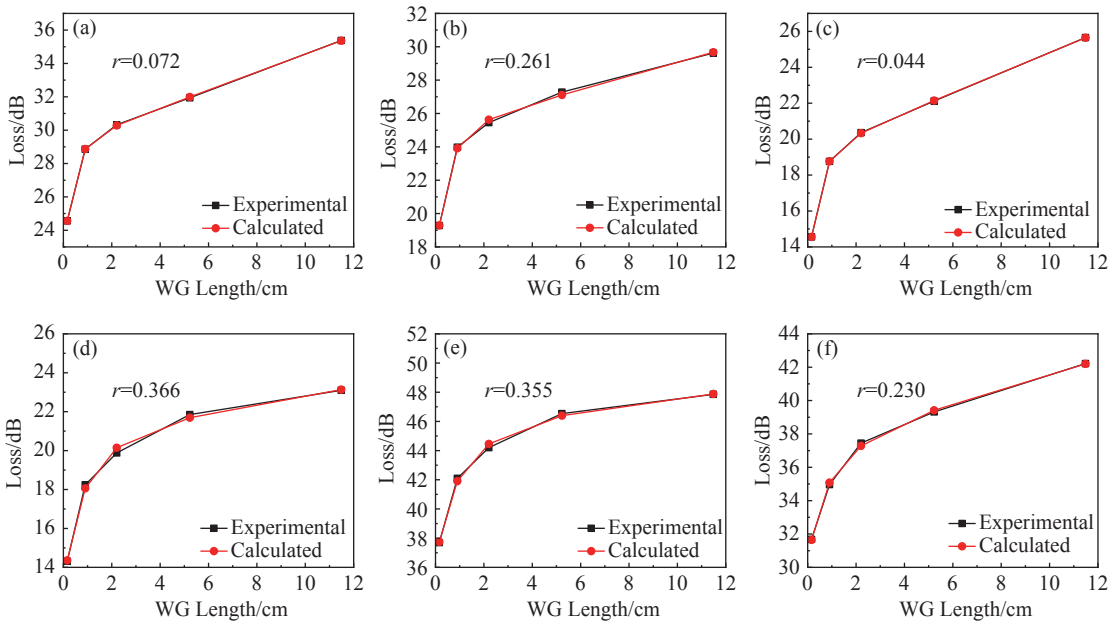

Fig. 7 The measurement results of the cut-back structure and the fitting results. (a) GC1, (b) GC2, (c) GC3, (d) GC4, (e) GC5-1, (f) GC5-2

Tab. 2 The summary of the fitting results

	α(dB/cm)	α_{b0}(dB)	k	α_{gc}(dB)	r
GC1	0.538	0.805	0.0446	20.220	0.072
GC2	0.408	0.698	0.0346	15.448	0.261
GC3	0.558	0.698	0.0399	10.740	0.044
GC4	0.209	0.393	0.0201	12.114	0.366
GC5-1	0.194	0.416	0.0176	35.350	0.355
GC5-2	0.421	0.339	0.0194	29.666	0.230

Tab. 3 The performance comparison of different measurement methods

	Advantages	Disadvantages
Traditional cut-back[33]	Widely employed owing to its ease of use.	Can't simultaneously measure the propagation loss and bending loss; Requires identical coupling conditions.
Three-prism Method[34]	Does not require constant coupling conditions	Has low measurement accuracy.
Fabry-Perot transmission method[35]	Can eliminate the influence of coupling loss and has higher accuracy	Requires a complex coupling system.
This paper	Can simultaneously measure waveguide propagation loss and bending loss; Smaller footprint; Simple and convenient operation.	

5 Conclusions

In this paper, we suggested a method to measure propagation loss, bending loss and coupling loss with a cut-back structure, in which the bending loss is expressed exponentially with the bending radius. Through the fitting method based on GA, we got the loss specifications of the fabricated LN waveguides. Finally, a propagation loss of 0.558 dB/cm, a bending loss of 0.698 dB/90° at 100 μm and a coupling loss of 10.74 dB were realized with square root r of only 0.044, which showed a close match with the test results. With this method, we can use a single cut-back structure to measure propagation loss and bending loss without using a large bending radius in the traditional cut-back structure. It will save significantly on the footprint without limiting the bending radius. We can simultaneously measure waveguide propagation loss and bending loss with this method.

References:

[1] ARIZMENDI L. Photonic applications of lithium niobate crystals[J]. *Physica Status Solidi (A)*, 2004, 201(2): 253-283.

[2] WEIS R S, GAYLORD T K. Lithium niobate: summary of physical properties and crystal structure[J]. *Applied Physics A*, 1985, 37(4): 191-203.

[3] WU R B, WANG M, XU J, *et al*... Long low-loss-litium niobate on insulator waveguides with sub-nanometer surface roughness[J]. *Nanomaterials*, 2018, 8(11): 910.

[4] ZHU D, SHAO L B, YU M J, *et al*... Integrated photonics on thin-film lithium niobate[J]. *Advances in Optics and Photonics*, 2021, 13(2): 242-352.

[5] RABIEI P, GUNTER P. Optical and electro-optical properties of submicrometer lithium niobate slab waveguides prepared by crystal ion slicing and wafer bonding[J]. *Applied Physics Letters*, 2004, 85(20): 4603-4605.

[6] POBERAJ G, HU H, SOHLER W, *et al*... Lithium niobate on insulator (LNOI) for micro-photonic devices[J]. *Laser & Photonics Reviews*, 2012, 6(4): 488-503.

[7] LEVY M, RADOJEVIC A M. Single-crystal lithium niobate films by crystal ion slicing[M]//ALEXE M, GÖSELE U. Wafer Bonding: Applications and Technology. Berlin: Springer, 2004: 417-450.

[8] ZHANG M, BUSCAINO B, WANG CH, *et al*... Broadband electro-optic frequency comb generation in a lithium niobate microring resonator[J]. *Nature*, 2019, 568(7752): 373-377.

[9] XU M Y, HE M B, ZHANG H G, *et al*... High-performance coherent optical modulators based on thin-film lithium niobate platform[J]. *Nature Communications*, 2020, 11(1): 3911.

[10] WANG CH, ZHANG M, CHEN X, *et al*... Integrated lithium niobate electro-optic modulators operating at CMOS-compatible voltages[J]. *Nature*, 2018, 562(7725): 101-104.

[11] WANG CH, LANGROCK C, MARANDI A, *et al*... Ultrahigh-efficiency wavelength conversion in nanophotonic periodically poled lithium niobate waveguides[J]. *Optica*, 2018, 5(11): 1438-1441.

[12] LIN J T, YAO N, HAO ZH ZH, *et al*... Broadband quasi-phase-matched harmonic generation in an on-chip

monocrystalline lithium niobate microdisk resonator[J]. *Physical Review Letters*, 2019, 122(17): 173903.

[13] HE M B, XU M Y, REN Y X, *et al*... High-performance hybrid silicon and lithium niobate Mach–Zehnder modulators for 100 Gbit s^{-1} and beyond[J]. *Nature Photonics*, 2019, 13(5): 359-364.

[14] CAI L T, KONG R R, WANG Y W, *et al*... Channel waveguides and y-junctions in x-cut single-crystal lithium niobate thin film[J]. *Optics Express*, 2015, 23(22): 29211-29221.

[15] CAI L T, WANG Y W, HU H. Low-loss waveguides in a single-crystal lithium niobate thin film[J]. *Optics Letters*, 2015, 40(13): 3013-3016.

[16] HU H, YANG J, GUI L, *et al*... Lithium niobate-on-insulator (LNOI): status and perspectives[J]. *Proceedings of SPIE*, 2012, 8431: 84311D.

[17] KRASNOKUTSKA I, TAMBASCO J L J, LI X J, *et al*... Ultra-low loss photonic circuits in lithium niobate on insulator[J]. *Optics Express*, 2018, 26(2): 897-904.

[18] ULLIAC G, COURJAL N, CHONG H M H, *et al*... Batch process for the fabrication of $LiNbO_3$ photonic crystals using proton exchange followed by CHF_3 reactive ion etching[J]. *Optical Materials*, 2008, 31(2): 196-200.

[19] DONG P, QIAN W, LIAO SH R, *et al*... Low loss shallow-ridge silicon waveguides[J]. *Optics Express*, 2010, 18(14): 14474-14479.

[20] GUTIERREZ A M, BRIMONT A, AAMER M, *et al*... Method for measuring waveguide propagation losses by means of a Mach–Zehnder Interferometer structure[J]. *Optics Communications*, 2012, 285(6): 1144-1147.

[21] TAEBI S, KHORASANINEJAD M, SAINI S S. Modified fabry-perot interferometric method for waveguide loss measurement[J]. *Applied Optics*, 2008, 47(35): 6625-6630.

[22] HE Y M, LI ZH S, LU D. A waveguide loss measurement method based on the reflected interferometric pattern of a Fabry-Perot cavity[J]. *Proceedings of SPIE*, 2018, 10535: 105351U.

[23] HOLLAND J H. *Adaptation in Natural and Artificial Systems: An Introductory Analysis with Applications to Biology, Control, and Artificial Intelligence*[M]. Cambridge: The MIT Press, 1992.

[24] ALONSO J M, ALVARRUIZ F, DESANTES J M, *et al*... Combining neural networks and genetic algorithms to predict and reduce diesel engine emissions[J]. *IEEE Transactions on Evolutionary Computation*, 2007, 11(1): 46-55.

[25] VERMA R, LAKSHMINIARAYANAN P A. A case study on the application of a genetic algorithm for optimization of engine parameters[J]. *Proceedings of the Institution of Mechanical Engineers*, *Part D*: *Journal of Automobile Engineering*, 2006, 220(4): 471-479.

[26] BAHADORI M, NIKDAST M, CHENG Q X, *et al*... Universal design of waveguide bends in silicon-on-insulator photonics platform[J]. *Journal of Lightwave Technology*, 2019, 37(13): 3044-3054.

[27] THYAGARAJAN K, SHENOY M R, GHATAK A K. Accurate numerical method for the calculation of bending loss in optical waveguides using a matrix approach[J]. *Optics Letters*, 1987, 12(4): 296-298.

[28] HAN ZH H, ZHANG P, BOZHEVOLNYI S I. Calculation of bending losses for highly confined modes of optical waveguides with transformation optics[J]. *Optics Letters*, 2013, 38(11): 1778-1780.

[29] STENGER V E, TONEY J, PONICK A, *et al*.. Low loss and low vpi thin film lithium niobate on quartz electro-optic modulators[C]. *2017 European Conference on Optical Communication* (*ECOC*), IEEE, 2017: 1-3.

[30] LI X P, CHEN K X, HU ZH F. Low-loss bent channel waveguides in lithium niobate thin film by proton exchange and dry etching[J]. *Optical Materials Express*, 2018, 8(5): 1322-1327.

[31] REN T H, ZHANG M, WANG CH, *et al*... An integrated low-voltage broadband lithium niobate phase modulator[J]. *IEEE Photonics Technology Letters*, 2019, 31(11): 889-892.

[32] DING T T, ZHENG Y L, CHEN X F. On-chip solc-type polarization control and wavelength filtering utilizing periodically poled lithium niobate on insulator ridge waveguide[J]. *Journal of Lightwave Technology*, 2019, 37(4): 1296-1300.

[33] VLASOV Y A, MCNAB S J. Losses in single-mode silicon-on-insulator strip waveguides and bends[J]. *Optics Express*, 2004, 12(8): 1622-1631.

[34] WON Y H, JAUSSAUD P C, CHARTIER G H. Three-prism loss measurements of optical waveguides[J]. *Applied Physics Letters*, 1980, 37(3): 269-271.

[35] REGENER R, SOHLER W. Loss in low-finesse Ti: $LiNbO_3$ optical waveguide resonators[J]. *Applied Physics B*, 1985, 36(3): 143-147.

Author Biographics：

Fan Zuowen (1998—), male, from Taian, Shandong Province, obtained his bachelors degree from Shandong University of Technology in 2016, and is a postgraduate student in the Microelectronics Institute, Shanghai University. He is mainly engaged in silicon photonics. E-mail: fanzuowen@shu.edu.cn

Jia Lianxi (1982 —), male, from Zibo, Shandong Province, professor, obtained a bachelors degree from Shandong University in 2005, and a doctorate degree from the Institute of Semiconductors, Chinese Academy of Sciences in 2010. He is mainly engaged in silicon photonics. E-mail: jialx@mail.sim.ac.cn